Article

# Versatile Synthesis Strategy for Carboxylic Acid–functionalized Upconverting Nanophosphors as Biological Labels

Zhigang Chen, Huili Chen, He Hu, Mengxiao Yu, Fuyou Li, Qiang Zhang, Zhiguo Zhou, Tao Yi, and Chunhui Huang

*J. Am. Chem. Soc.*, **2008**, 130 (10), 3023-3029 • DOI: 10.1021/ja076151k



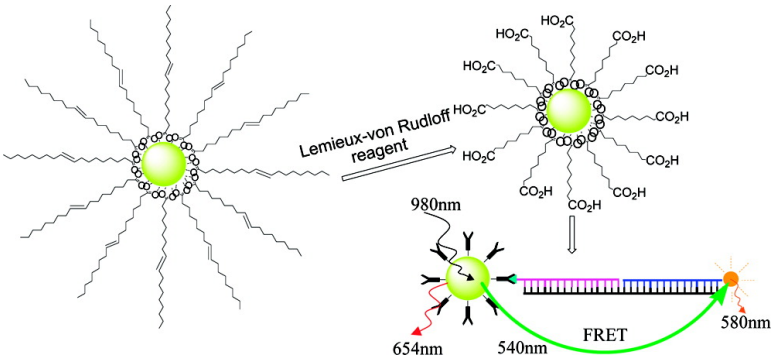


## More About This Article

Additional resources and features associated with this article are available within the HTML version:

- Supporting Information
- Links to the 8 articles that cite this article, as of the time of this article download
- Access to high resolution figures
- Links to articles and content related to this article
- Copyright permission to reproduce figures and/or text from this article

View the Full Text HTML

J|A|C|S
ARTICLES
Published on Web 02/16/2008

# Versatile Synthesis Strategy for Carboxylic Acid−functionalized Upconverting Nanophosphors as Biological Labels

Zhigang Chen, Huili Chen, He Hu, Mengxiao Yu, Fuyou Li,* Qiang Zhang, Zhiguo Zhou, Tao Yi, and Chunhui Huang*

*Department of Chemistry & Laboratory of Advanced Materials, Fudan University, 220 Handan Road, Shanghai 200433, People's Republic of China*

Received August 15, 2007; E-mail: fyli@fudan.edu.cn; chhuang@pku.edu.cn

***Abstract:*** Up-converting rare-earth nanophosphors (UCNPs) have great potential to revolutionize biological luminescent labels, but their use has been limited by difficulties in obtaining UCNPs that are biocompatible. To address this problem, we have developed a simple and versatile strategy for converting hydrophobic UCNPs into water-soluble and carboxylic acid-functionalized analogues by directly oxidizing oleic acid ligands with the Lemieux-von Rudloff reagent. This oxidation process has no obvious adverse effects on the morphologies, phases, compositions and luminescent capabilities of UCNPs. Furthermore, as revealed by Fourier transform infrared (FTIR) and NMR results, oleic acid ligands on the surface of UCNPs can be oxidized into azelaic acids ($HOOC(CH_2)_7COOH$), which results in the generation of free carboxylic acid groups on the surface. The presence of free carboxylic acid groups not only confers high solubility in water, but also allows further conjugation with biomolecules such as streptavidin. A highly sensitive DNA sensor based on such streptavidin-coupled UCNPs have been prepared, and the demonstrated results suggest that these biocompatible UCNPs have great superiority as luminescent labeling materials for biological applications.

## 1. Introduction

Conventional downconversion fluorescent materials, including organic dyes,[1] semiconductor nanocrystals (such as CdS, CdSe, CdTe),[2] and dye-coupled hybrid materials (carbon nanotubes[3] and mesoporous silica[4]), are the commonly used fluorophores for biological studies and clinical application due to their unique features. However, they also have many intrinsic limitations. Organic dyes have a number of known drawbacks, such as weak photostability, and broad absorption and emission bands.[1] Semiconductor nanocrystals are still controversial due to their inherent toxicity and chemical instability, although they exhibit high photostability, size-dependent emissions, high quantum yields, and narrow emission bands.[5] In addition, these down-conversion fluorescent materials usually emit one lower-energy photon after absorption of a higher-energy ultraviolet (UV) or visible photon. The use of higher-energy light is associated with several significant disadvantages, such as low light-penetration depth, possible severe photodamage to living organisms, and the autofluorescence (noise) of some biological samples. Although some organic dyes and semiconductor nanocrystals can emit higher-energy photons through two-photo absorption processes, quantum efficiencies are very low and an expensive pulsed laser is necessary.[6] To solve these problems, the development of alternative biological luminescent labels through the use of up-converting rare-earth nanophosphors (UCNPs) has attracted a tremendous amount of attention due to the unique luminescence properties of rare-earth nanocrystals, such as sharp absorption and emission lines, high quantum yields, long lifetimes, and superior photostability.[7] In particular, upconversion is a process where low-energy light, usually near-infrared (NIR) or infrared (IR), is converted to higher-energy light (UV

(1) (a) Miyawaki, A.; Sawano, A.; Kogure, T. *Nature Cell Biol.* **2003**, *5* (suppl.), S1−S7. (b) Holmes, K. L.; Lantz, L. M. *Methods Cell Biol.* **2001**, *63*, 185−204. (c) Banks, P. R.; Paquette, D. M. *Bioconjugate Chem.* **1995**, *6*, 447−458. (d) Zhang, M.; Yu, M. X.; Li, F. Y.; Zhu, M. W.; Li, M. Y.; Gao, Y. H.; Li, L.; Liu, Z. Q.; Zhang, J. P.; Zhang, D. Q.; Yi, T.; Huang, C. H. *J. Am. Chem. Soc.* **2007**, *129*, 10322−10323.

(2) (a) Bruchez, M., Jr.; Moronne, M.; Gin, P.; Weiss, S.; Alivisatos, A. P. *Science* **1998**, *281*, 2013−2016. (b). Chan, W. C. W.; Nie, S. *Science* **1998**, *281*, 2016−2018. (c) Dubertret, B.; Skourides, P.; Norris, D. J.; Noireaux, V.; Brivanlou, A. H.; Libchaber, A. *Science* **2002**, *298*, 1759−1762. (d) Medintz, I. L.; Uyeda, H. T.; Goldman, E. R.; Mattoussi, H. *Nature Mater.* **2005**, *4*, 435−446. (e) Michalet, X.; Pinaud, F. F.; Bentolila, L. A.; Tsay, J. M.; Doose, S.; Li, J. J.; Sundaresan, G.; Wu, A. M.; Gambhir, S. S.; Weiss, S. *Science* **2005**, *307*, 538−544. (f) Zhou, D. J.; Piper, J. D.; Abell, C.; Klenerman, D.; Kang, D. J.; Ying, L. M. *Chem. Commun.* **2005**, 4807−4089.

(3) For recent examples: (a) Becker, M. L.; Fagan, J. A.; Gallant, N. D.; Bauer, B. J.; Bajpai, V.; Hobbie, E. K.; Lacerda, S. H.; Migler, K. B.; Jakupciak, J. P. *Adv. Mater.* **2007**, *19*, 939−945. (b) Liu, Z.; Cai, W. B.; He, L. N.; Nakayama, N.; Chen, K.; Sun, X. M.; Chen, X. Y.; Dai, H. J. *Nature Nanotechnology* **2007**, *2*, 47−52. (c) Nakayama-Ratchford, N.; Bangsaruntip, S.; Sun, X. M.; Welsher, K.; Dai, H. J. *J. Am. Chem. Soc.* **2007**, *129*, 2448−2449. (d) Kostarelos, K.; Lacerda, L.; Pastorin, G.; Wu, W.; Wieckowski, S.; Luangsivilay, J.; Godefroy, S.; Pantarotto, D.; Briand, J. P.; Muller, S.; Prato, M.; Bianco, A. *Nature Nanotechnol.* **2007**, *2*, 108−113.

(4) a) Slowing, I. I.; Trewyn, B. G.; Lin, V. S.-Y. *J. Am. Chem. Soc.* **2007**, *129*, 8845−8849. b) Torney, F.; Trewyn, B. G.; Lin, V. S.-Y.; Wang, K. *Nature Nanotechnol.* **2007**, *2*, 295−300.

(5) Wang, F.; Tan, W. B.; Zhang, Y.; Fan, X.; Wang, M. *Nanotechnology* **2006**, *17*, R1−R13.

(6) a) Denk, W.; Strickler, J. H.; Webb, W. W. *Science* **1990**, *248*, 73−76. b) Larson, D. R.; Zipfel, W. R.; Williams, R. M.; Clark, S. W.; Bruchez, M. P.; Wise, F. W.; Webb, W. W. *Science* **2003**, *300*, 1434−1437.

or visible), through multiple photon absorptions or energy transfers.[8] In comparison with downconversion fluorescent materials, up-converting rare-earth materials have many advantages in biological applications, such as noninvasive and deep penetration of NIR radiation, the absence of autofluorescence of biological tissues, and feasibility of multiple labeling by UCNPs with different emissions under the same excitation.[7] Unfortunately, despite recent advances in the synthetic methods for controlling the size and shape of UCNPs,[9−11] the UCNPs with hydrophobic organic ligands (such as oleic acid) coating their surface cannot be used directly in biological applications because of their very low solubility in water and unfavorable surface properties. So, a prerequisite for the development of UCNP-based biological labels is to gain access to water-soluble nanoparticles bearing appropriate functional groups (such as −COOH, $-NH_2$, or −SH) on their surface for conjugation of biomolecules.

Generally, some applications of nanosized materials greatly depend on surface functionalization, and two main strategies have been developed for converting hydrophobic nanocrystals (including semiconductor and rare-earth materials) into ones that can be dispersed in water and also have some functional chemical groups on their surfaces. One strategy is based on the encapsulation of hydrophobic nanocrystals with $SiO_2$[2a,2d,2e,7b,7e,9a,12] or amphiphilic copolymer.[2c,2d,7a,13] However, these processes may be costly and/or complicated, and precise control of some factors (such as the thickness of encapsulation layer) may be difficult. For example, Zhang et al.[14] reported a useful approach for preparing biocompatible silica-coated polyvinylpyrrolidone/$NaYF_4$ nanocrystals, but it was found that several $NaYF_4$ nanocrystals could be easily incorporated into one silica shell, probably resulting in some difficulties in biological applications. The other strategy involves replacing the original organic layer with hydrophilic ligands.[2b,2d,2e,15] For example, Doris et al.[16] recently reported a versatile strategy for semiconductor quantum-dot ligand exchange. However, up to now, no approach involving ligand exchange for the preparation of water-soluble and functionalized UCNPs has been reported, owing to difficulties in obtaining versatile substitutional ligands. Therefore, it is necessary to develop new and simple methods for synthesizing hydrophilic and functionalized UCNPs.

To date, oleic acid, containing a −CH═CH− group, has been widely used as the capping ligand in most successful synthesis approaches to UCNPs[9a,9d,10] and other nanocrystals.[17] The Lemieux−von Rudloff oxidation method is well-known to oxidize selectively a carbon−carbon double bond (R−CH═CH−R′) to give two carboxylic acids.[18] These features trigger our interest in the novel concept of converting hydrophobic UCNPs into hydrophilic ones. Herein, we introduce a new, simple and versatile strategy for synthesizing water-soluble and carboxylic acid-functionalized UCNPs by directly oxidizing oleic acid ligands to azelaic acid ($HOOC(CH_2)_7COOH$) with the Lemieux−von Rudloff reagent. Moreover, owing to the presence of free carboxylic acid groups on their surface, the oxidized UCNPs can be directly conjugated with proteins (such as streptavidin). A DNA sensor based on streptavidin-coupled UCNPs has been successfully fabricated.

## 2. Experimental Section

**2.1. Materials.** All of the chemicals used were of analytical grade and were used without further purification. NaOH, NaF, ethanol, *tert*-butanol, $K_2CO_3$, cyclohexane, acetone, hydrochloric solution, $KMnO_4$, and $NaIO_4$ were purchased from Sinopharm Chemical Reagent Co. (China). Oleic acid was obtained from Alfa Aesar. Rare earth chlorides ($LnCl_3$, Ln: Y, Yb, Er, Ho, Tm) were prepared by dissolving the corresponding oxides ($Y_2O_3$, $Yb_2O_3$, $Er_2O_3$, $Ho_2O_3$, and $Tm_2O_3$ from Beijing Lansu Co. China) in 10% hydrochloric solution and then evaporating the water completely.

The oligonucleotides 5′-(biotin)-GATGAGTATTGATGC−3′ (as Capture-DNA), 5′-CGAATAGTTCCATTG−(TAMRA)-3′ (as Report-DNA) and 5′-CAATGGAACTATTCG GCATCAATACTCATC-3′ (as Target-DNA) were purchased from Sangon Biotechnology Co. Ltd of Shanghai, China. Lysine, 1-ethyl-3-(3-dimethylaminopropyl)carbodiimide hydrochloride (abbreviated as EDC), *N*-hydroxysulfosuccinimide sodium salt (abbreviated as sulfo-NHS), morpholine ethanesulfonic acid (abbreviated as MES) and tris(hydroxymethyl)methanamine (abbreviated as Tris) were obtained from Sinopharm Chemical Reagent Co. (China).

**2.2. Synthesis of Upconverting Nanophosphors. 2.2.1. Synthesis of Oleic Acid-Capped UCNPs.** Various UCNPs were prepared by a modified hydrothermal process.[9a] In a typical synthesis, NaOH (1.2 g, 30 mmol), water (9 mL), ethanol (10 mL), and oleic acid (20 mL) were mixed under agitation to form a homogeneous solution. Then 0.6 mmol (total amounts) of rare-earth chloride (1.2 mL, 0.5 mol/L $LnCl_3$, Ln: Y or 78 mol%Y + 20 mol%Yb + 2 mol%Er (Ho or Tm)) aqueous solution was added under magnetic stirring. Subsequently, 1.0 M aqueous NaF (4 mL) solution was added dropwise to the above solution. The mixture was agitated for about 10 min, then transferred to a 50 mL autoclave, sealed, and hydrothermally treated at 160 °C for 8 h. The system was cooled to room-temperature naturally, and the products


(7) (a) Wang, L. Y.; Yan, R. X.; Hao, Z. Y.; Wang, L.; Zeng, J. H.; Bao, J.; Wang, X.; Peng, Q.; Li, Y. D. *Angew. Chem., Int. Ed.* **2005**, *44*, 6054−6057. (b) Yi, G. S.; Lu, H. C.; Zhao, S. Y.; Yue, G.; Yang, W. J.; Chen, D. P.; Guo, L. H. *Nano Lett.* **2004**, *4*, 2191−2196. (c) Lim, S. F.; Riehn, R.; Ryu, W. S.; Khanarian, N.; Tung, C.-k.; Tank, D.; Austin, R. H. *Nano Lett.* **2006**, *6*, 169−174. (d) Kuningas, K.; Ukonaho, T.; Pakkila, H.; Rantanen, T.; Rosenberg, J.; Lovgren, T.; Soukka, T. *Anal. Chem.* **2006**, *78*, 4690−4696. (e) Zhang, P.; Rogelj, S.; Nguyen, K.; Wheeler, D. *J. Am. Chem. Soc.* **2006**, *128*, 12410−12411.

(8) Auzel, F. *Chem. Rev.* **2004**, *104*, 139−173.

(9) (a) Wang, L. Y.; Li, Y. D. *Chem. Mater.* **2007**, *19*, 727−734. (b) Wang, X.; Zhuang, J.; Peng, Q.; Li, Y. D. *Inorg. Chem.* **2006**, *45*, 6661−6665. (c) Wang, X.; Zhuang, J.; Peng, Q.; Li, Y. D. *Nature* **2005**, *437*, 121−124. (d) Wang, L. Y.; Li, Y. D. *Nano Lett.* **2006**, *6*, 1645−1649.

(10) (a) Mai, H. X.; Zhang, Y. W.; Si, R.; Yan, Z. G.; Sun, L. D.; You, L. P.; Yan, C. H. *J. Am. Chem. Soc.* **2006**, *128*, 6426−6436. (b) Yi, G. S.; Chow, G. M. *Adv. Funct. Mater.* **2006**, *16*, 2324−2329. (c) Boyer, J. C.; Vetrone, F.; Cuccia, L. A.; Capobianco, J. A. *J. Am.Chem. Soc.* **2006**, *128*, 7444−7445.

(11) (a) Heer, S.; Kompe, K.; Gudel, H. U.; Haase, M. *Adv. Mater.* **2004**, *16*, 2102−2105. (b) Lehmann, O.; Meyssamy, H.; Kompe, K.; Schnablegger, H.; Haase, M. *J. Phys. Chem. B* **2003**, *107*, 7449−7453. (c) Heer, S.; Lehmann, O.; Haase, M.; Güdel, H.-U. *Angew. Chem., Int. Ed.* **2003**, *42*, 3179−3182.

(12) (a) Schroedter, A.; Weller, H.; Eritja, R.; Ford, W. E.; Wessels, J. M. *Nano Lett.* **2002**, *2*, 1363−1367. (b) Zhelev, Z.; Ohba, H.; Bakalova, R. *J. Am. Chem. Soc.* **2006**, *128*, 6324−6325. (c) Zhang, T.; Stilwell, J. L.; Gerion, D.; Ding, L.; Elboudwarej, O.; Cooke, P. A.; Gray, J. W.; Alivisatos, A. P.; Chen, F. F. *Nano Lett.* **2006**, *6*, 800−808. (d) Rieter, W. J.; Taylor, K. M. L.; Lin, W. *J. Am. Chem. Soc.* **2007**, *129*, 9852−9853.

(13) Yi, G. S.; Chow, G. M. *Chem. Mater.* **2007**, *19*, 341−343.

(14) Li, Z.; Zhang, Y. *Angew. Chem., Int. Ed.* **2006**, *45*, 7732−7735.

(15) (a) Kim, S.; Bawendi, M. G. *J. Am. Chem. Soc.* **2003**, *125*, 14652−14653. (b) Wang, Y. A.; Li, J. J.; Chen, H.; Peng, X. *J. Am. Chem. Soc.* **2002**, *124*, 2293−2298.

(16) Dubois, F.; Mahler, B.; Dubertret, B.; Doris, E.; Mioskowski, C. *J. Am. Chem. Soc.* **2007**, *129*, 482−483.

(17) (a) Park, J.; An, K.; Hwang, Y.; Park, J.-G.; Noh, H.-J.; Kim, J.-Y.; Park, J.-H.; Hwang, N.-M.; Hyeon, T. *Nature Mater.* **2004**, *3*, 891−895. (b) Yu, W. W.; Peng, X. *Angew. Chem., Int. Ed.* **2002**, *41*, 2368−2371. (c) Pradhan, N.; Reifsnyder, D.; Xie, R.; Aldana, J.; Peng, X. *J. Am. Chem. Soc.* **2007**, *129*, 9500−9509. (d) Park, J.; Joo, J.; Kwon, S. G.; Jang, Y.; Hyeon. T. *Angew. Chem., Int. Ed.* **2007**, *46*, 4630−4660. (e) Chaubey, G. S.; Barcena, C.; Poudyal, N.; Rong, C.; Gao, J.; Sun, S.; Liu, J. P. *J. Am. Chem. Soc.* **2007**, *129*, 7214−7215. (f) Wang, C.; Daimon, H.; Lee, Y.; Kim, J.; Sun, S. *J. Am. Chem. Soc.* **2007**, *129*, 6974−6975.

(18) (a) Lemieux, R. U.; von Rudloff, E. *Can. J. Chem.* **1955**, *33*, 1701−1709. (b) Higashimura, T.; Sawamoto, M.; Hiza, T.; Karaiwa, M.; Tsuchii, A.; Suzuki, T. *Appl. Environ. Microb.* **1983**, *46*, 386.

were deposited at the bottom of the vessel. Cyclohexane was used to dissolve and collect the products. The products were subsequently deposited by adding ethanol to the sample-containing cyclohexane solution. The resulting mixture was then centrifuged to obtain powder samples. Pure powders could be obtained by purifying the samples with ethanol several times to remove oleic acid, sodium oleic, and other remnants.

**2.2.2. Converting Hydrophobic UCNPs into Hydrophilic Ones.** A mixture of as-prepared UCNP sample (0.1 g), cyclohexane (100 mL), *tert*-butanol (70 mL), water (10 mL) and 5 wt % $K_2CO_3$ aqueous solution (5 mL) were stirred at room temperature for about 20 min. Then 20 mL of Lemieux−von Rudloff reagent (5.7 mM $KMnO_4$ and 0.105 M $NaIO_4$ aqueous solution[18]) was added dropwise. The resulting mixture was stirred at about 40 °C for over 48 h. The product was then isolated by centrifugation and washed with deionized water, acetone, and ethanol. Subsequently, the product was dispersed in hydrochloric acid (50 mL) of pH 4−5, and the mixture was stirred for 30 min. At last, the oxidized product was obtained by centrifugation, washed twice with deionized water and dried under vacuum.

**2.3. Preparation of a DNA Sensor. 2.3.1. Preparation of Streptavidin-Functionalized UCNPs.** To activate the surface carboxylic acid groups,[19] EDC (5 mg, $2.6\times10^{-5}$ mol) and sulfo-NHS (15 mg, $6.9\times10^{-5}$ mol) were added to MES buffer (0.1 M, 20 mL, pH 6.0) containing the oxidized $NaYF_4$:Yb,Er nanoparticles (5 mg). The mixture was then stirred for 8 h at room temperature. After centrifugation and washed with water, the precipitate was added into PBS buffer solution (0.1 M, 5 mL, pH 7.2) containing streptavidin (2 mg, $\sim3\times10^{-8}$ mol). The linkage reaction was allowed to proceed at 4 °C for 48 h. Then lysine (20 mg, $1.4\times10^{-4}$ mol) was added to remove any unreacted sulfo-NHS. Finally, streptavidin-functionalized $NaYF_4$:Yb,Er nanoparticles were obtained by centrifugation, and washed three times with water.

**2.3.2. Detection of DNA.** The sensor system consisted of streptavidin-functionalized UCNPs (0.1 mg/mL), Report-DNA (100 nM) and Capture-DNA (100 nM) in a buffered (100 mM Tris-HCl, 3 mM $MgCl_2$, pH 8.0) solution. The detecting experiment was performed by keeping the concentration of sensor constant while varying the concentration of Target-DNA. Aliquots of stock solutions of Target-DNA were titrated into the above solution. After each addition of Target-DNA, the mixture was stirred at 37 °C for 20 min to facilitate the hybridization reaction. After slowly cooling to room temperature (25 °C), the luminescence spectrum of the system was measured under continuous-wave excitation at 980 nm.

**2.4. Characterization.** Sizes and morphologies of UCNPs were determined at 200 kV using a JEOL JEM-2010F high-resolution transmission electron microscope (HR-TEM). Samples of the as-prepared and oxidized UCNPs were prepared by placing a drop of dilute dispersions in cyclohexane and ethanol, respectively, on the surface of a copper grid. Energy-dispersive X-ray analysis (EDXA) of the samples was also performed during HR-TEM measurements. X-ray diffraction (XRD) measurements were made with a Bruker D4 X-ray diffractometer using Cu K$\alpha$ radiation ($\lambda$ = 0.15418 nm). $^1$H NMR spectra were recorded on a Varian Mercury 400 spectrometer. Proton chemical shifts are reported in ppm downfield from tetramethylsilane (TMS). Fourier transform infrared (FT-IR) spectra were measured using an IRPRESTIGE-21 spectrometer (Shimadzu) from samples in KBr pellets. Thermogravimetric analysis (TGA) curves were recorded on a DTG-60H (Shimadzu) at a heating rate of 10 °C/min. Dynamic light scattering (DLS) experiments were carried out on an ALV-5000 spectrometer-goniometer equipped with an ALV/LSE-5004 light scattering electronic and multiple tau digital correlator and a JDS Uniphase He−Ne laser (632.8 nm) with an output power of 22 mW. To ensure the accuracy of DLS measurement, great care was taken to eliminate dust from the samples. The aqueous solution of the oxidized UCNPs was filtered through two membrane filters with 0.45 $\mu$m nominal pore size connected in series. The size distribution was measured at 25 °C with a detection angle of 90°. Luminescence spectra were measured with an Edinburgh LFS-920 fluorescence spectrometer. Up-conversion fluorescence spectra were obtained using an external 0−800 mW adjustable continuous-wave laser (980 nm, Beijing Hi-Tech Optoelectronic Co., China) as the excitation source, instead of the Xenon source in the spectrophotometer. UV−visible absorption spectra were measured using a Shimadzu UV-2550 ultraviolet−visible-near-infrared spectrophotometer.

## 3. Results and Discussion

**3.1. Synthesis and Characterization of UCNPs.** In the present work, $NaYF_4$: 20 mol%Yb, 2 mol % Er (Tm or Ho), was synthesized by a hydrothermal route in the presence of oleic acid, since $NaYF_4$ has been reported to be the most efficient host material for Yb/Er (or Yb/Tm or Yb/Ho) co-doped NIR-to-visible upconversion phosphors.[20] In the course of the reaction, oleic acid molecules were coated onto the outer face of the in-situ generated UCNPs through the interaction between rare-earth ions ($Ln^{3+}$) and carboxyl groups of oleic acids, with the hydrophobic alkyl chains left outside.[9,10] All as-prepared samples were easily dispersed in a nonpolar solvent (such as hexane or chloroform) and then deposited by the addition of a polar solvent (such as ethanol or acetone). To convert hydrophobic oleic acid-capped UCNPs into carboxylic acid-functionalized derivatives, we used the Lemieux−von Rudloff reagent to oxidize the as-prepared samples (Figure 1).

Figure 2 presents representative TEM images of the as-prepared and oxidized $NaYF_4$:Yb,Er samples. The monodisperse nanocubes of the as-prepared samples with sizes of 8−14 nm suggest that the long-chain oleic acid ligands on the crystal surface prevent aggregation (Figure 2A). After the Lemieux−von Rudloff oxidation, the oxidized samples were seen to still consist primarily of single nanocubes, but the formation of nanoarrays was prevented due to interaction effects of the oxidized ligands (Figure 2B). Both samples exhibit very similar particle size distributions (10.8 ± 1.3 nm, s.d.: 4.2% for the as-prepared sample and 4.5% for the oxidized sample, as shown in Figure S1 of the Supporting Information). Similar TEM results were also observed for other samples ($NaYF_4$:Yb,Tm and $NaYF_4$:Yb,Ho as shown in Figure S2 and S3 of the Supporting Information). These observations show that such oxidation has no obvious effects on the size and shape of UCNPs except for their array. In this respect, our oxidation method has an advantage over other strategies; for example, the previously reported encapsulation strategy (with $SiO_2$ or amphiphilic copolymer) usually increases the particle size and changes the shape of nanocrystals.

EDXA patterns and XRD patterns of both the as-prepared and oxidized $NaYF_4$:Yb,Er samples were also studied to investigate the effects of the oxidation process. EDXA patterns (Figure S4 of the Supporting Information) confirm the presence of Na, Y, Yb, and F in both samples, and no obvious changes in the composition are observed. XRD patterns (Figure S5 of the Supporting Information) also demonstrate that both samples have similar phases (dominant cubic phase accompanied by small amounts of hexagonal phase). Therefore, it can be concluded that the oxidation has no obvious adverse effects on the compositions and phases of UCNPs.

(19) Dumelin, C. E.; Scheuermann, J.; Melkko, S.; Neri, D. *Bioconjugate Chem.* **2006**, *17*, 366−370.

(20) Kramer, K. W.; Biner, D.; Frei, G.; Gudel, H. U.; Hehlen, M. P.; Luthi, S. R. *Chem. Mater.* **2004**, *16*, 1244−1251.

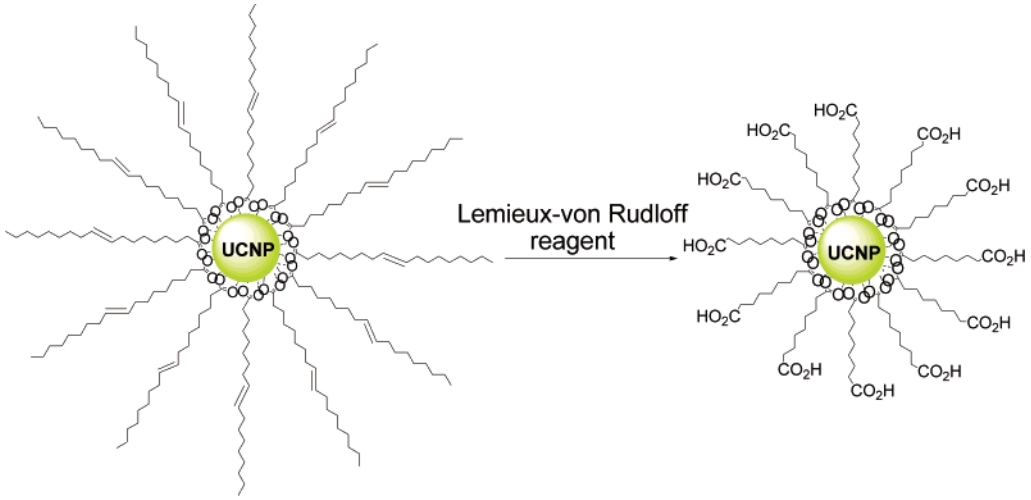


***Figure 1.*** Synthesis mechanism of carboxylic acid-functionalized UCNPs from oleic acid-capped precursors.

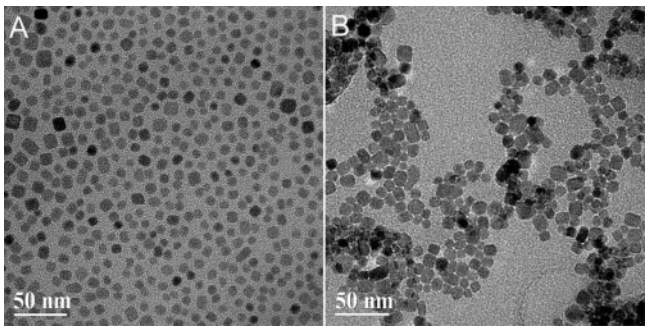


***Figure 2.*** TEM images of the as-prepared (A) and oxidized (B) $NaYF_4$:Yb,Er samples.

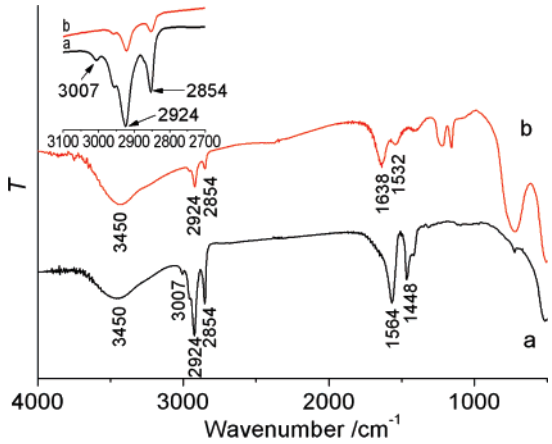


***Figure 3.*** FTIR spectra of the as-prepared (a) and oxidized (b) $NaYF_4$:Yb,Er samples.

The capping ligands on the surface of UCNPs were identified by FT−IR spectra (Figure 3). Both the as-prepared and oxidized $NaYF_4$:Yb,Er samples exhibit a broad band at around 3450 $cm^{-1}$, corresponding to O−H stretching vibration. The transmission bands at 2924 and 2854 $cm^{-1}$ in both samples are respectively assigned to the asymmetric ($\upsilon_{as}$) and symmetric ($\upsilon_s$) stretching vibrations of methylene ($CH_2$) in the long alkyl chain.[9d] A peak at 3007 $cm^{-1}$ attributed to the =C−H stretching vibration can clearly be seen in the spectrum of the as-prepared sample (Figure 3a),[9d] but this feature is apparently lost in the spectrum of the oxidized sample (Figure 3b), suggesting cleavage of the −HC=CH− group. In addition, bands at 1564 and 1448 $cm^{-1}$ are also found in the spectrum of the as-prepared sample, associated with the asymmetric ($\upsilon_{as}$) and symmetric ($\upsilon_s$) stretching vibrations of the carboxylic group of the bound oleic acid. However, in the case of the oxidized sample, bands corresponding to the carboxylic group are observed at 1638 and 1532 $cm^{-1}$. The evolution of ligands on the surface was further investigated by $^1H$ NMR analysis of the undoped $NaYF_4$ samples (Figure S6 of the Supporting Information). The $^1H$ NMR spectrum (Figure S6A) of the as-prepared $NaYF_4$ sample dispersed in $CDCl_3$ is consistent with previously reported data for oleic acid-capped nanocrystals,[10] and thus confirms the presence of oleic acid ligands in the as-prepared samples. The $^1H$ NMR signals of the bound oleic acid molecules on the surface of nanoparticles are broadened with respect to those of the free oleic acid,[21a] which results from an inhomogeneous distribution of the magnetic environments due to site variations on the nanoparticle surface as well as a decrease in the rotational freedom of the ligands.[22] The $^1H$ NMR spectrum of the oxidized $NaYF_4$ sample dispersed in DMSO-$d_6$ was also recorded (Figure S6B), and proved to be similar to the standard spectrum of azelaic acid, apart from the broadening.[21b] In contrast, a peak centered at $\delta = 5.34$ ppm (peak d, assigned to −HC=CH−) and a peak centered at $\delta = 0.85$ ppm (peak a, assigned to $-CH_3$) disappeared after the oxidation, indicative of cleavage of the carbon−carbon double bond in oleic acid ligands. On the basis of the above-described FTIR and NMR results, it can be deduced that the oleic acid ligands on the surface of UCNPs are oxidized to azelaic acids.

To evaluate the ligand content in both the as-prepared and oxidized $NaYF_4$:Yb,Er samples, thermogravimetric analysis (TGA) was performed (Figure S7 of the Supporting Information). TGA curves show two weight loss stages in the range of 40 to 600 °C. The first weight loss stage in the temperature range of 40−200 °C is due to the loss (2−3 wt %) of absorbed water from both samples. The second stage from 200 to 600 °C is attributed to the combustion of the organic groups in the samples, and the weight loss in this stage reflects the ligand

(21) (a) Standard NMR of oleic acid: www.sigmaaldrich.com/spectra/ fnmr/FNMR004904.PDF; (b) Standard NMR of azelaic acid: www.sigmaaldrich.com/spectra/fnmr/FNMR004172.PDF.

(22) (a) Sudarsan, V.; Sivakumar, S.; van Veggel, F. C. J. M.; Raudsepp, M. *Chem. Mater.* **2005**, *17*, 4736−4742. (b) Kuno, M.; Lee, J. K.; Dabbousi, B. O.; Mikulec, F. V.; Bawendi, M. G. *J. Chem. Phys.* **1997**, *106*, 9869−9882.

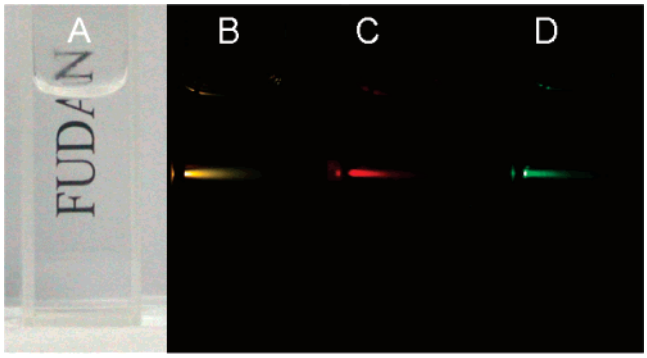


***Figure 4.*** Colloidal solutions of the oxidized $NaYF_4$: 20 mol%Yb, 2 mol % Er sample in water: (A) The solution showing its transparency; (B) Total upconversion under continuous-wave excitation at 980 nm; (C and D) upconversion viewed through red and green filters, respectively.

content. It is clear that the content of oleic acid ligands in the present as-prepared samples is about 11.32 wt %, and that the content of azelaic acid ligands decreases to 7.55 wt %, which chiefly results from the change in molecular weight of ligands (from 282.46 for oleic acid to 188.22 for azelaic acid). The results also suggest that almost all of the ligands are still attached to UCNPs during the oxidization.

As a result of the ligand evolution from oleic acid to azelaic acid on the surface of UCNPs, all of the oxidized samples can be readily dispersed in water (Figure 4A) and in some polar organic solvents such as DMF, or DMSO (Figure S8 of the Supporting Information) due to the presence of free carboxylic acid groups. Dynamic light scattering analysis (Figure S9 of the Supporting Information) further indicates that most of the oxidized UCNPs in aqueous solution are about 12.5 nm in diameter with excellent dispersion, and only a very small amount of UCNP aggregates of diameter 70−120 nm can be observed, correlating nicely with the particle size determined by TEM study (Figure 2B). The luminescent properties of the oxidized samples in water were investigated, and Figure 4B−D shows the upconversion luminescence photographs of a colloidal aqueous solution of the oxidized $NaYF_4$:20 mol%Yb, 2 mol % Er sample under continuous-wave excitation at 980 nm. The total luminescence (Figure 4B) appears yellow-green in color due to a combination of green and red emissions from the $Er^{3+}$ ion. This is confirmed by Figure 4, parts C and D, where the solution under the same excitation conditions is viewed through red and green filters, respectively. The corresponding upconversion spectrum of the oxidized sample in water and that of the as-prepared samples in cyclohexane under continuous-wave excitation at 980 nm are shown in Figure 5, and are similar to previously reported spectra for these materials.[10b,10c,11a,14] Both spectra feature three distinct $Er^{3+}$ emission bands. The green emissions between 514 and 534 nm and between 534 and 560 nm are the result of transitions from $^2H_{11/2}$ and $^4S_{3/2}$ to $^4I_{15/2}$ of $Er^{3+}$, respectively. A red emission is observed between 635 and 680 nm due to the transition from $^4F_{9/2}$ to $^4I_{15/2}$. It is well-known that the crystallinity and surface properties of UCNPs may alter the intensity of the fluorescence emission peaks of the doping lanthanide ions. For example, $NaYF_4$:Yb,Er samples prepared under different conditions exhibit different intensity ratios of the green and red emission peaks.[10b,10c,11a,14] In this case of $NaYF_4$:Yb,Er, a slight decrease in this ratio ($I_{540}/I_{654}$) is observed, from 0.93 for the as-prepared sample to 0.87 for the oxidized sample (Figure 5), which may be attributed to the

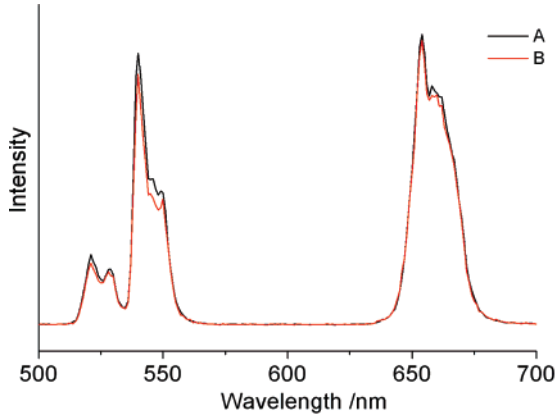


***Figure 5.*** Luminescence spectra of aqueous solutions of $NaYF_4$: 20 mol%Yb, 2 mol % Er nanoparticles (0.4 mg/mL) excited with a 980-nm laser: (A) As-prepared sample in cyclohexane; (B) the oxidized sample in water.

change of ligands. Similar effects are also found for other samples ($NaYF_4$:Yb,Tm and $NaYF_4$:Yb,Ho as shown in Figure S10 of the Supporting Information). In addition, colloidal aqueous solutions of UCNPs exhibit similar luminescent spectra as the pH of the solution is adjusted over a wide range (pH 2∼11, Figure S11 of the Supporting Information), indicating excellent pH-independent luminescent properties of UCNPs as compared to organic dyes and semiconductor quantum dots.[1,2]

**3.2. Applications as Luminescent Biological Labels.** Most importantly, the presence of free carboxylic acid groups on the surface of azelaic acid-capped UCNPs facilitates further conjugation with various biomolecules. Typically, the terminal carboxylic acid groups allow the immobilization of amine-containing proteins and DNA. In view of the highly specific interaction (high affinity, $K_d = 10^{-15}$) between streptavidin and biotin,[23] in the present study, streptavidin was chosen as the target biomacromolecule to attach to the oxidized UCNPs. As shown in Figure 6A, covalent coupling of streptavidin to the surface of UCNPs was facilitated by cross-linkers (EDC and sulfo-NHS) which activated the surface carboxy groups on UCNPs and led to the formation of amide bonds with streptavidin.

Furthermore, as an applied example of UCNP-based luminescent biological labels, the feasibility of designing a DNA sensor based on streptavidin−functionalized UCNPs was demonstrated through the specific interaction between streptavidin and biotin. The design principle of the DNA sensor is shown in Figure 6B. By using two shorter oligonucleotides to capture a longer target oligonucleotide, a sandwich-type hybridization format is adopted in this DNA sensor. One of the shorter oligonucleotides is labeled with biotin (DNA1-biotin, as capture-DNA) (Figure 6B), and the other is labeled with TAMRA (DNA2-TAMRA, as reporter-DNA) whose excitation spectrum overlies the green emission band of the $NaYF_4$:Yb,Er nanoparticles (Figure S12 of the Supporting Information). Under illumination with a 980-nm laser, only luminescent signals of $NaYF_4$:Yb,Er nanoparticles were observed from a mixture of DNA1-biotin, DNA2-TAMRA, and streptavidin-functionalized $NaYF_4$:Yb,Er nanoparticles (Figure 7A). This indicates that the nanoparticle and DNA2-TAMRA are far apart in the absence of target-DNA, and that energy transfer from the nanoparticles

(23) Wilchek, M.; Bayer, E. A. *Methods Enzymol.* **1990**, *184*, 14−45.

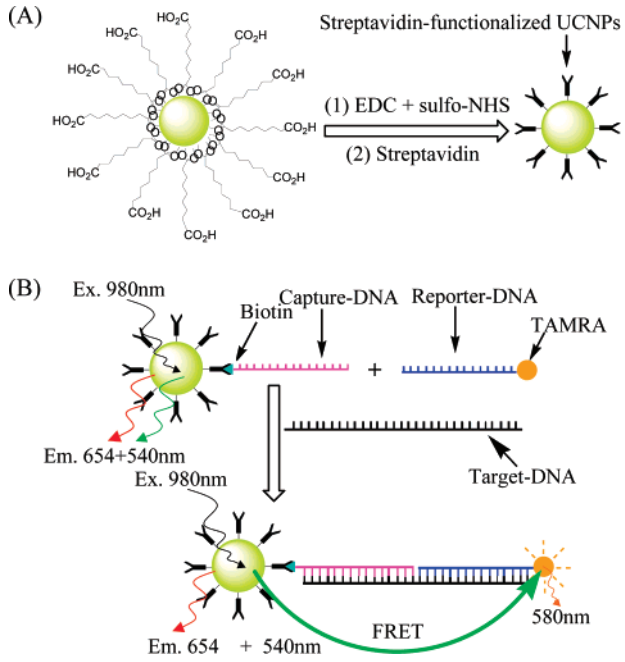


***Figure 6.*** Synthesis of streptavidin−functionalized UCNPs (A) and schematic of DNA nanosensors based on UCNPs (B).

to TAMRA is negligible under continuous-wave excitation at 980 nm. Upon addition of target-DNA, a broad and featureless emission band (∼580 nm) gradually appears, corresponding to the TAMRA emission, and signal intensities of green emissions between 514 and 560 nm of UCNPs decreases significantly while those of red emissions between 635 and 680 nm remain largely unchanged (Figure 7A), thus indicating energy transfer from the green emission of UCNPs to TAMRA. The effective energy transfer implies that the resulting assembly brings the fluorophore (energy acceptor) and the rare earth nanoparticle (energy donor) into close proximity. In addition, the luminescence intensity ratio ($I_{580}/I_{540}$ or $I_{540}/I_{654}$) is found to vary linearly with the concentration of target-DNA in the measured range of 10−50 nM (Figure 7, parts B and C), suggesting high sensitivity. Thus, we can quantitatively detect the target oligonucleotide by monitoring the intensity ratio upon continuous-wave excitation at 980 nm. The successful fabrication of a DNA sensor also indicates that streptavidin molecules on the surface of $NaYF_4$:Yb,Er nanoparticles remain highly active.

The highly specific interaction between streptavidin and biotin has been widely applied in the studies of modern biological and medical fields,[24] and a wide variety of biotinylation reagents are commercially available.[25] Consequently, streptavidin-functionalized UCNPs may be used for detecting and/or binding to a broad range of biotinylated proteins and DNA. Therefore, we anticipate that this streptavidin coating surface chemistry provides a novel approach for the production of biocompatible photoluminescent UCNP probes, giving UCNPs great potential as luminescent labeling materials for biological applications.

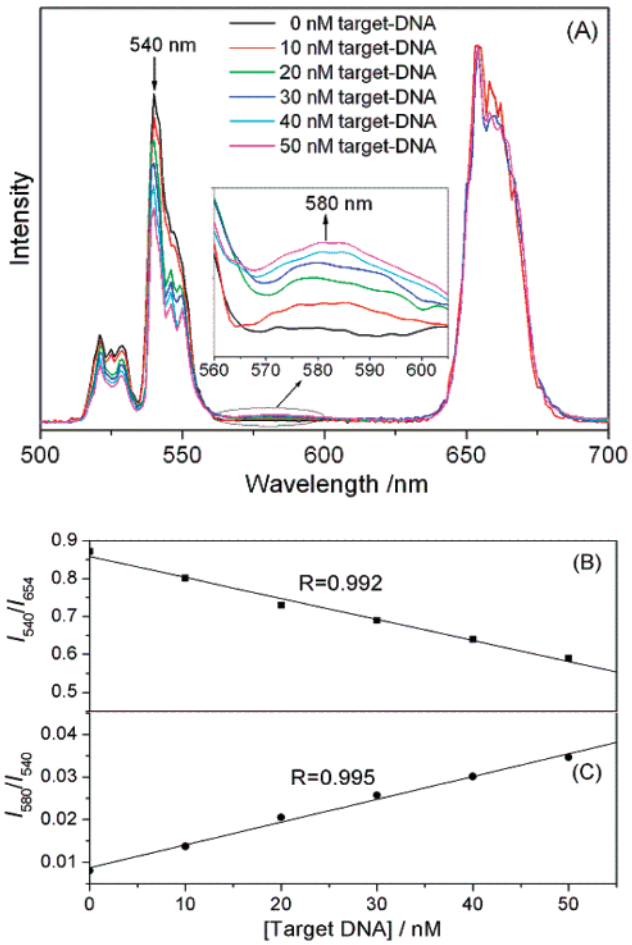


***Figure 7.*** Luminescence spectra of a mixture of streptavidin-functionalized $NaYF_4$:Yb,Er nanoparticles, capture-DNA, and reporter-DNA in the presence of different concentrations of target-DNA under continuous-wave excitation at 980 nm (A), and the linear relationships between target-DNA concentration and the intensity ratios $I_{540}/I_{654}$ (B) or $I_{580}/I_{540}$ (C).

## 4. Conclusions

In summary, we have demonstrated a new, efficient and versatile procedure for converting hydrophobic UCNPs into water-soluble and carboxylic acid-functionalized derivatives by directly oxidizing oleic acid ligands to azelaic acid. No obvious adverse effects of the oxidation on the morphologies, phases, compositions and upconversion luminescence of UCNPs are observed. It should be noted that our conversion procedure is very simply, and do not change the size and shape of particles in contrast with the previously reported encapsulation strategy. Moreover, this procedure is not limited to hydrophobic UCNPs, and it can easily be applied to other hydrophobic nanoparticles (including rare earth, semiconductor and metal nanoparticles) where only surface ligands can be oxidized.

More importantly, the presence of free carboxylic acid groups on the surface of azelaic acid-capped UCNPs allows further conjugation with various biomolecules, and streptavidin-functionalized UCNPs derived from azelaic acid-capped precursors provides a novel approach for detecting and/or binding to a broad range of biotinylated proteins or antibodies. The successful fabrication of a DNA sensor based on streptavidin-functionalized UCNPs suggests that it might be possible to expand the application of these UCNPs as luminescent labels into other biological fields such as bioimaging.

(24) (a) Pinaud, F.; King, D.; Moore, H.-P.; Weiss, S. *J. Am. Chem. Soc.* **2004**, *126*, 6115−6123. (b) Ramanathan, K.; Bangar, M. A.; Yun, M.; Chen, W.; Myung, N. V.; Mulchandani, A. *J. Am. Chem. Soc.* **2005**, *127*, 496−497. (c) Oh, E.; Hong, M.-Y.; Lee, D.; Nam, S.-H.; Yoon, H. C.; Kim, H.-S. *J. Am. Chem. Soc.* **2005**, *127*, 3270−3271. (d) Zhang, C.-Y.; Yeh, H.-C.; Kuroki, M. T.; Wang, T.-H. *Nature Mater.* **2005**, *4*, 826−931.

(25) For example, see: www.invitrogen.com.

**Acknowledgment.** The authors thank National High Technology Program of China (2006AA03Z318), National Science Foundation of China (20490210 and 20501006) and Shanghai Sci. Tech. Comm. (05DJ14004 and 06QH14002) for financial support.

**Supporting Information Available:** Size distribution, TEM characterization, EDXA spectra, XRD patterns, TGA curves and luminescence spectra of UCNPs; $^1$H NMR spectra of the undoped $NaYF_4$; Photographs of colloidal solutions of UCNPs in DMF and DMSO; absorption and emission spectra of aqueous solution of TARMA-labeled reporter DNA. This material is available free of charge via the Internet at http://pubs.acs.org.

JA076151K